Parity Nonconservation in Neutron Resonances in 133Cs

E I. Sharapov
Joint Institute for Nuclear Research

J D. Bowman
Los Alamos National Laboratory

Bret E. Crawford
Gettysburg College

See next page for additional authors

Parity Nonconservation in Neutron Resonances in 133Cs

Abstract

Spatial parity nonconservation (PNC) has been studied in the compound-nuclear states of ^{134}Cs by measuring the helicity dependence of the neutron total cross section. Transmission measurements on a thick ^{133}Cs target were performed by the time-of-flight method at the Manuel Lujan Neutron Scattering Center with a longitudinally polarized neutron beam in the energy range from 5 to 400 eV. A total of 28 new p-wave resonances were found, their neutron widths determined, and the PNC longitudinal asymmetries of the resonance cross sections measured. The value obtained for the root-mean-square PNC element $M=(0.06_{-0.02}^{+0.25})$ meV in ^{133}Cs is the smallest among all targets studied. This value corresponds to a weak spreading width $\Gamma_w=(0.006_{-0.003}^{+0.154})\times10^{-7}$ eV.

Disciplines

Atomic, Molecular and Optical Physics | Physics

Authors

E I. Sharapov, J D. Bowman, Bret E. Crawford, P P J. Delheij, T Haseyama, J N. Knudsen, L Y. Lowie, A Masaike, Y Matsuda, G E. Mitchell, S I. Penttila, H Postma, N R. Roberson, S J. Seestrom, Sharon L. Stephenson, Y-F Yen, and V W. Yuan

Parity nonconservation in neutron resonances in ^{133}Cs

E. I. Sharapov,[1] J. D. Bowman,[2] B. E. Crawford,[3,*] P. P. J. Delheij,[4] T. Haseyama,[5] J. N. Knudson,[2] L. Y. Lowie,[6,†] A. Masaike,[5,‡] Y. Masuda,[7] Y. Matsuda,[5,§] G. E. Mitchell,[6] S. I. Penttilä,[2] H. Postma,[8] N. R. Roberson,[3] S. J. Seestrom,[2] S. L. Stephenson,[6,‖] Y.-F. Yen,[2,¶] and V. W. Yuan[2]

[1]*Joint Institute for Nuclear Research, 141980 Dubna, Russia*
[2]*Los Alamos National Laboratory, Los Alamos, New Mexico 87545*
[3]*Duke University, Durham, North Carolina 27708 and Triangle Universities Nuclear Laboratory, Durham, North Carolina 27708-0308*
[4]*TRIUMF, Vancouver, British Columbia, Canada V6T 2A3*
[5]*Physics Department, Kyoto University, Kyoto 606-01, Japan*
[6]*North Carolina State University, Raleigh, North Carolina 27695-8202 and Triangle Universities Nuclear Laboratory, Durham, North Carolina 27708-0308*
[7]*National Laboratory of High Energy Physics, Tsukuba-shi, 305, Japan*
[8]*Delft University of Technology, Delft, 2600 GA, The Netherlands*

(Received 19 October 1998)

Spatial parity nonconservation (PNC) has been studied in the compound-nuclear states of ^{134}Cs by measuring the helicity dependence of the neutron total cross section. Transmission measurements on a thick ^{133}Cs target were performed by the time-of-flight method at the Manuel Lujan Neutron Scattering Center with a longitudinally polarized neutron beam in the energy range from 5 to 400 eV. A total of 28 new p-wave resonances were found, their neutron widths determined, and the PNC longitudinal asymmetries of the resonance cross sections measured. The value obtained for the root-mean-square PNC element $M=(0.06^{+0.25}_{-0.02})$ meV in ^{133}Cs is the smallest among all targets studied. This value corresponds to a weak spreading width $\Gamma_w=(0.006^{+0.154}_{-0.003})\times 10^{-7}$ eV. [S0556-2813(99)03503-7]

PACS number(s): 24.80.+y, 25.40.Ny, 27.60.+j, 11.30.Er

I. INTRODUCTION

Parity violation (PV) research in nuclear physics has always pursued two goals: the study of the fundamental weak interaction itself and, as stressed in a new review [1], application of PV for improved understanding of nuclear structure and nuclear reactions. The discovery of a large enhancement for the parity nonconservation (PNC) signal in neutron p-wave resonances by the Dubna group [2] opened new possibilities for development in this field. The best method to study parity violation in the compound nucleus is the transmission measurement of longitudinally polarized neutrons through an isotopically pure target. The quantities measured in such experiments are the longitudinal asymmetries of cross sections for p-wave resonances, defined as $\sigma_p^{\pm}=\sigma_p(1\pm p)$, where $\sigma_p^{\pm}$ is the resonance cross section for $+$ and $-$ neutron helicities, and σ_p is the resonance part of the p-wave cross section. The Time Reversal Invariance and Parity at Low Energies (TRIPLE) Collaboration initiated a program to study parity violation in the compound nucleus using the high epithermal neutron flux available at the Manuel Lujan Neutron Scattering Center at the Los Alamos Neutron Science Center (LANSCE). The TRIPLE Collaboration developed new techniques to produce and utilize a longitudinally polarized beam of resonance neutrons and measured a number of PNC asymmetries in each of several nuclides. The status of our earlier measurements is summarized by Bowman *et al.* [3] and by Frankle *et al.* [4]. Recently the TRIPLE Collaboration has published new PNC results for ^{238}U [5], ^{232}Th [6], ^{113}Cd [7], ^{107}Ag and ^{109}Ag [8], and ^{93}Nb [9].

One milestone was the development of a statistical approach to the analysis of the PNC data [10,11]. The TRIPLE Collaboration introduced a new procedure to extract the root-mean-square matrix element of the weak interaction (and the weak spreading width in the compound nucleus) from the measured PNC asymmetries of neutron cross sections. The details of this analysis are given by Bowman *et al.* [12]. In this new approach the symmetry-breaking matrix elements V_{ik}, which connect the ith p-wave resonance with the kth s-wave resonance of the same spin J, are random variables with mean value zero and variance $\overline{v^2_{M_J}}$. Experimental PNC asymmetries p_i are realizations of a Gaussian variable with variance $\overline{v^2_p}$. It was shown that

$$\overline{v_p^2}=\mathcal{E}\left\{\sum_k A_{ik}^2\right\}\overline{v^2_{M_J}}, \tag{1}$$

where the expectation value $\mathcal{E}$ is taken with respect to both i and k ensembles and the so-called ''amplification param-

*Present address: North Carolina State University, Raleigh, NC 27695-8202 and Gettysburg College, Gettysburg, PA 17325.
†Present address: McKinsey and Company, Atlanta, GA 30303.
‡Present address: Fukui University of Technology, 3-6-1 Gakuen, Fukui, Japan.
§Present address: Institute of Physical and Chemical Research (RIKEN), Saitama, 351-0198, Japan.
‖Present address: Gettysburg College, Gettysburg, PA 17325.
¶Present address: Wake Forest University School of Medicine, Winston-Salem, NC 27157.

eters'' $A_{ik}^2 = 4\Gamma_{nk}/[\Gamma_{ni}(E_k - E_i)^2]$ are determined for each resonance. This equation and the definition

$$M_J \equiv \sqrt{\overline{v_{M_J}^2}} \tag{2}$$

permit extraction of the root-mean-square matrix element M_J from the PNC asymmetries p. In practice, likelihood analysis is used to obtain M_J [12]. Conversely, one can use Eq. (1) to estimate the size of PNC longitudinal asymmetries: $p = \sqrt{\overline{v_p^2}} = (0.2-10)\%$ for a typical value of $M_J \simeq 2$ meV and a range of values (1–50) eV^{-1} for A_{ik}. Because the mean-square matrix element $\overline{v_p^2}$ is expected [13] to be proportional to the mean level spacing D_J, it is customary to introduce the weak spreading width

$$\Gamma_w = 2\pi M_J^2/D_J, \tag{3}$$

which has a typical value of $\sim 10^{-7}$ eV. One expects that the spreading width for any symmetry-breaking interaction is approximately the same for all nuclei. We note that local fluctuations have been observed in the spreading width for isotopic spin mixing [14]. One major goal of the present work and of other experiments by the TRIPLE Collaboration is to measure the weak interaction spreading width for a numder of nuclei and to determine the global and local properties of the weak spreading width.

For low energy neutrons the p-wave resonance neutron widths are very small. Our previous studies of the mass dependence of parity violation were performed for targets with masses $A \sim 100$ and $A \sim 230$. These targets are close to the $3p$ and $4p$ neutron strength function maxima. Only near these strength function maxima can p-wave resonances be observed and studied with satisfactory precision. However, in order to observe possible local fluctuations, it is important to extend measurements for targets away from these neutron strength function maxima. This was one of the motivations for our choice of cesium as a target for PV study. Cesium has only one stable isotope, ^{133}Cs, with nearly the same (~ 20 eV) s-wave spacing as ^{238}U and almost no known p-wave resonances [15]. We felt that the apparent absence of p-wave resonances in cesium was due to the insufficient sensitivity of previous measurements, the latest of which was published in 1977 [16]. Our interpretation proved correct: we observed 28 extremely weak p-wave resonances up to 400 eV. In many cases, the neutron spectroscopic analysis of the observed p-wave resonances led to large amplification parameters A_{ik} favorable for PNC. However, the experimental longitudinal asymmetries have rather small values. From this result, the conclusion is that cesium has an exceptionally small value of the weak matrix element M and the spreading width Γ_w.

II. EXPERIMENTAL METHOD

The experiment was performed by the time-of-flight method at the pulsed spallation neutron source [17] of the Manuel Lujan Neutron Scattering Center at the Los Alamos Neutron Science Center. We refer to earlier papers [5–9] for a detailed description of the experimental method; here we provide only a brief summary. Transmission data on a thick cesium target were measured with a longitudinally polarized neutron beam. The neutron beam was 70% polarized by transmission through a polarized proton target. The protons in frozen ammonia were polarized by the dynamic polarization process at 1-K temperature in a 5-T field of a split-coil superconducting magnet. The proton polarization direction relative to the polarizing magnetic field (positive and negative proton polarization) was reversed every few days. The neutron spin direction parallel or antiparallel to the neutron beam momentum (positive or negative helicity state) was rapidly reversed by an adiabatic spin flipper in an eight-step sequence with each spin state lasting 10 s. This sequence was designed to reduce the effects of gain drifts and residual transverse magnetic fields. The neutron beam intensity was monitored by a pair of ^{3}He and ^{4}He ionization chambers and the neutron polarization was monitored by NMR measurement of the proton polarization. The absolute value of the neutron beam polarization was obtained from PV measurements with a lanthanum sample by normalizing to the well-known longitudinal asymmetry [18] for the 0.73-eV resonance in ^{139}La.

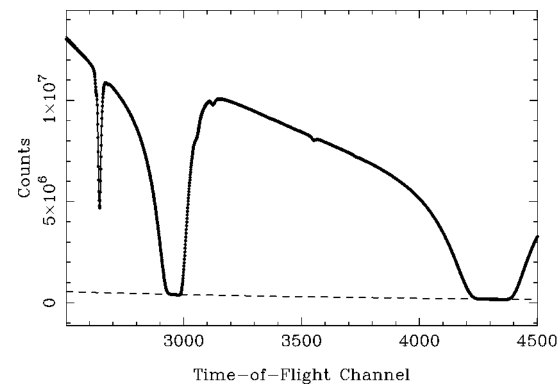

FIG. 1. The time-of-flight spectrum for ^{133}Cs for the energy region from 22 eV to 79 eV. The channel width is 200 ns and the detector counts are summed for two helicity states over 45 runs.

Care was taken to remove the water of hydration from the CsF which was canned in a hermetically sealed environment. The 99.999% chemically pure target of CsF was contained in an aluminum cylinder of length 29.80 cm and diameter 11.50 cm. The target mass was 6338 g, which corresponds to an areal density of 2.42×10^{23} cesium atoms/cm^2. Neutrons were detected at 56.74 m from the source by a large ^{10}B-loaded liquid scintillation detector segmented into 55 cells. The 55 separately discriminated signals were linearly summed. An analog-to-digital converter (ADC) transient recorder was used to sample the summed signal in 8192 time-of-flight channels of 200-ns width. After 20 eight-step sequences, the data from this approximately 30-minute period were stored as a ''run.'' In the final data analysis 104 runs with positive proton polarization and 90 runs with negative proton polarization were used. A sample of a neutron time-of-flight spectrum for 45 runs is shown in Fig. 1. As can be seen in Fig. 1, the spectrum contains exceptionally small transmission dips. We list all of them in Sec. III, Table I. We do not include resonances from the latest measurements on cesium [16]. Resonances in Table I are either known or new resonances in cesium or resonances in target contaminants. In the latter case, the peaks should correspond to strong reso-

TABLE I. Neutron resonance parameters for ^{133}Cs.

E (eV)	$g\Gamma_n$ (meV)	l	J [a]	$A_{J=3}$ (1/eV)	$A_{J=4}$ (1/eV)
5.91 ± 0.01	3.23 ± 0.15	0	3		
9.50 ± 0.01	$(0.95\pm0.10)\times10^{-3}$	1	3	38.0	9.6
16.77 ± 0.02 [b]	$(0.77\pm0.08)\times10^{-4}$	1		88.8	34.2
18.86 ± 0.02 [b]	$(0.68\pm0.09)\times10^{-4}$	1		133	36.7
19.98 ± 0.02 [b]	$(0.38\pm0.04)\times10^{-3}$	1		79.4	15.8
22.52 ± 0.02	3.38 ± 0.20	0	3		
30.00 ± 0.03 [b]	$(0.55\pm0.07)\times10^{-4}$	1			
33.00 ± 0.03 [b]	$(2.90\pm0.40)\times10^{-4}$	1		35.7	18.2
42.75 ± 0.04 [b]	$(0.65\pm0.08)\times10^{-3}$	1		49.0	12.4
44.63 ± 0.04 [b]	$(3.40\pm0.40)\times10^{-3}$	1		34.9	54.6
47.52 ± 0.04	8.72 ± 0.71	0	3		
58.09 ± 0.04 [b]	$(0.4\pm0.1)\times10^{-3}$	1		51.4	17.3
59.61 ± 0.04	$(0.36\pm0.10)\times10^{-1}$	1			
60.24 ± 0.04 [b]	$(1.95\pm0.23)\times10^{-3}$	1		44.4	7.90
78.52 ± 0.05 [b]	$(0.50\pm0.07)\times10^{-3}$	1		22.4	24.6
80.00 ± 0.05 [b]	$(1.54\pm0.25)\times10^{-3}$	1		13.6	15.6
82.71 ± 0.05	3.18 ± 0.47	0	4		
88.96 ± 0.06 [b]	$(1.60\pm0.13)\times10^{-2}$	1		10.3	23.0
94.21 ± 0.06	11.6 ± 1.0	0			
110.45 ± 0.07 [b]	$(0.16\pm0.02)\times10^{-2}$	1		8.8	18.9
115.00 ± 0.07 [b]	$(0.41\pm0.05)\times10^{-2}$	1		5.7	20.4
117.51 ± 0.07 [b]	$(0.40\pm0.06)\times10^{-2}$	1		7.5	37.3
119.92 ± 0.08 [b]	$(5.40\pm0.45)\times10^{-2}$	1		1.6	86.7
126.1 ± 0.09	58.6 ± 0.5	0	4		
140.0 ± 0.1	3.72 ± 0.35	0	3		
146.0 ± 0.1	13.6 ± 1.2	0	4		
155.3 ± 0.1 [b]	$(0.88\pm0.09)\times10^{-1}$	1		1.2	7.2
167.0 ± 0.1 [b]	$(0.20\pm0.02)\times10^{-1}$	1		1.9	5.2
181.5 ± 0.1	1.04 ± 0.11	0	3		
201.1 ± 0.2	10.6 ± 1.0	0	4		
207.5 ± 0.2	2.08 ± 0.21	0	4		
217.1 ± 0.2 [b]	0.27 ± 0.03	0	4		
220.5 ± 0.2	11.1 ± 1.3	0	4		
234.1 ± 0.2	193.3 ± 15.0	0	4		
238.4 ± 0.2	7.0 ± 0.8	0	4		
267.5 ± 0.2 [b]	$(8.2\pm1.0)\times10^{-2}$	1		0.7	3.8
271.0 ± 0.2 [b]	$(3.6\pm0.5)\times10^{-2}$	1		1.2	5.7
273.6 ± 0.3 [b]	$(1.40\pm0.13)\times10^{-2}$	1		2.1	9.0
284.9 ± 0.3 [b]	$(12.6\pm1.1)\times10^{-2}$	1		2.2	4.3
288.4 ± 0.3 [b]	$(28.6\pm3.1)\times10^{-2}$	0			
295.5 ± 0.3	61.2 ± 6.0	0	4		
312.0 ± 0.3 [b]	$(4.0\pm0.4)\times10^{-2}$	1			
324.0 ± 0.3 [b]	$(3.0\pm0.4)\times10^{-2}$	1			
328.0 ± 0.3 [b]	$(3.0\pm0.4)\times10^{-1}$	1			
330.2 ± 0.3 [b]	$(1.6\pm0.2)\times10^{-1}$	1			
359.1 ± 0.4	18.6 ± 1.6	0	4		
362.8 ± 0.4 [b]	$(1.6\pm0.2)\times10^{-1}$	1			
377.1 ± 0.4	8.9 ± 0.9	0	3		
386.3 ± 0.4 [b]	$(0.30\pm0.03)\times10^{-1}$	1			
400.5 ± 0.4	132.0 ± 18.0	0			

[a] J values from [15].

[b] New resonances.

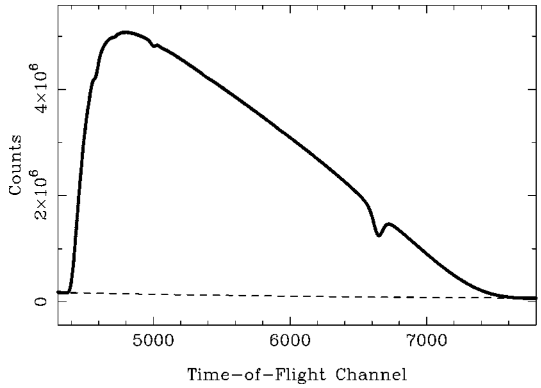

FIG. 2. Sample fit (solid line) to a time-of-flight spectrum (points) for the energy region from 5.9 eV to 22.5 eV. The dashed line is the background. The chi-square value per the degree of freedom is about 1.2 when fitted in the limited range of chanels around the 9.5-eV resonance.

nances. We checked the energies and strengths against all known strong resonances in other elements [15] and concluded that the newly observed weak dips belong to cesium. It is not surprising that they were not observed earlier [16], because we used a sample about 10 times thicker than in the previous measurements and the spallation source at LANSCE produced a much more intense neutron beam.

III. *p*-WAVE RESONANCES IN ^{133}Cs

After correction for dead time count losses, the experimental spectra were analyzed to obtain resonance parameters E_0 and $g\Gamma_n$ using the multilevel fitting code FITXS [19] developed for fitting time-of-flight (TOF) spectra measured at the LANSCE pulsed spallation neutron source. Details of the fitting procedures are given by Matsuda [20] and by Crawford *et al.* [21]. The final fitting function is written as

$$\mathcal{F}_t(t)=\left[B_t(t)\otimes\left(\frac{\alpha}{E^{\beta}}e^{-n\sigma_D(t)}\right)\right]+\sum_{i=0}^{3}\frac{a_i}{t^i}. \qquad (4)$$

Here $\sigma_D(t)$ is the Doppler-broadened total cross section for *s*- and *p*-wave resonances written using the Reich-Moore approximation [22]. $B_t(t)$ is the instrumental response function, which includes line broadening due to the initial width of the proton pulse, neutron moderation time in the water moderator, finite TOF channel width, and time of the neutron moderation in the ^{10}B-loaded liquid scintillator before capture by boron-10. The energy dependence of the neutron flux at epithermal energies is given by α/E^{β}. The second term on the right side of Eq. (4) represents a polynomial fit to the background. The symbol $\otimes$ indicates a convolution. Sample multilevel fits are shown in Figs. 1 and 2.

The resonance parameters were determined by fitting the time-of-flight spectra summed for both helicity states. Since the initial time-of-flight spectra were taken with unknown detector efficiency and neutron flux, a normalization procedure was performed using known resonance parameters [15] for several low-energy cesium resonances. This procedure was the main source of the systematic uncertainty of 9% in our $g\Gamma_n$ values. The neutron energy scale was calibrated against the resonance energies of ^{232} listed in Ref. [15]. The

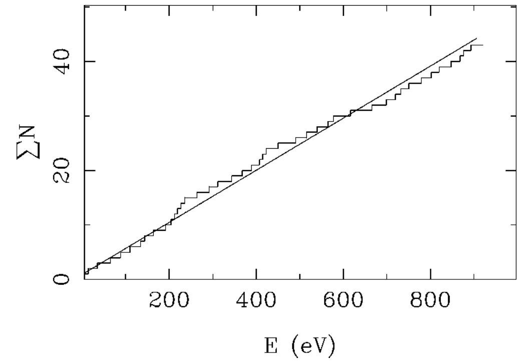

FIG. 3. Cumulative number of levels for ^{133}Cs *s*-wave resonances. A linear fit was used to extract the *s*-wave level spacing.

resulting resonance energies of ^{133}Cs have better accuracy than in previous measurements. Most of the *s*-wave resonance parameters agree with those given in the compilation by Mughabghab *et al.* [15]. For new resonances we assigned the orbital angular momentum *l* probabilistically, following Bollinger and Thomas [23]. This procedure applies the Bayes theorem to the Porter-Thomas distributions of neutron widths for *s*- and *p*-wave resonances. Our application of this procedure is described in Ref. [21].

Our resonance parameters are listed in Table I. The resonance energy, neutron width, orbital angular momentum *l*, and total angular momentum *J* are given for all resonances for which they were measured, while the quantity $A_i=\Sigma_k A_{ik}^2$ is listed for those *p*-wave resonances for which the longitudinal asymmetry was measured. Because the spins of the *p*-wave resonances are unknown, there are two entries for A_i corresponding to spins $J=3$ and $J=4$ for which mixing of *p*- and *s*-wave levels by the weak interaction is possible. The A_i values are zero for spins $J=2$ and $J=5$ because such *p*-wave resonances cannot exhibit parity violation. The amplification parameters A_i for cesium *p*-wave resonances have nearly the same size as for A_i *p*-wave resonances in ^{232}Th [6]. The large values of the amplification parameters make ^{133}Cs a good candidate for PNC study.

Before describing the PNC data analysis we first consider the neutron spectroscopic results. Figures 3 and 4 show the cumulative number of levels and Figs. 5 and 6 the cumulative reduced neutron width distributions for the *s*- and *p*-wave resonances. Both *s*-wave distributions have a typical

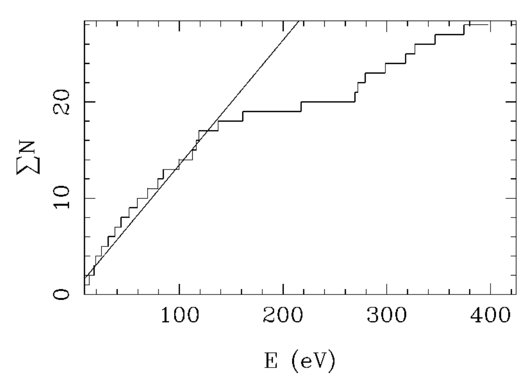

FIG. 4. Cumulative number of levels for ^{133}Cs *p*-wave resonances. The linear fit indicates that some levels are missed above 120 eV.

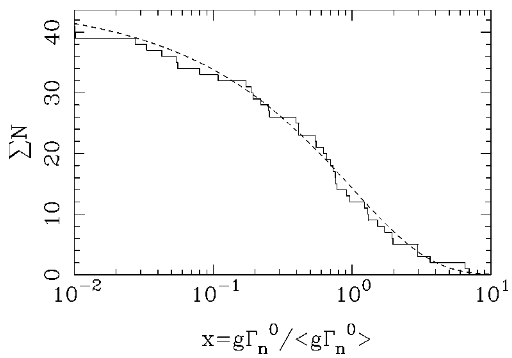

FIG. 5. Integrated reduced-neutron width distribution for *s*-wave resonances in cesium up to 800 eV. The dashed line is the Porter-Thomas distribution.

shape, while the plot of the cumulative number of levels for the *p*-wave resonances indicates that some levels are being missed above 120 eV. The *p*-wave reduced width distribution in the limited energy region up to 120 eV is reasonable considering the relatively small number of levels involved. From linear least-squares fits of the curves in Figs. 3 and 4 the average *s*- and *p*-wave level spacings were determined to be 20.5 ± 1.9 eV and 8.0 ± 1.0 eV, respectively. Neutron strength functions were obtained from these data according to the definition

$$S_l=\frac{\Sigma g\Gamma_n^l}{(2l+1)\Delta E}, \tag{5}$$

where the summation is over the reduced neutron widths $g\Gamma_n^l$ values in the energy interval ΔE and l is the orbital momentum ($l=0$ for *s* waves and $l=1$ for *p* waves). The results are $S_0=(0.80\pm0.17)\times10^{-4}$ and $S_1=(1.1\pm0.3)\times10^{-4}$. The value of the *p*-wave neutron strength function for cesium was not known prior to the present measurement. We include the present value in the plot in Fig. 7, which shows the mass dependence of the *p*-wave strength function versus A in the vicinity of the $3p$ strength function maximum. Data from Ref. [15] are supplemented with results from the TRIPLE spectroscopic studies of neutron *p*-wave resonances. Cesium has the lowest value of the *p*-wave strength function S_1 among nuclei studied by the TRIPLE Collaboration. In this mass region, the spin-orbit interaction influences the $S^1_{j=1/2}$ and $S^1_{j=3/2}$ components of the *p*-wave strength function [24]:

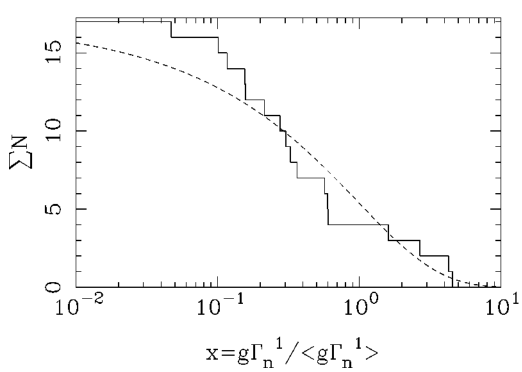

FIG. 6. Integrated reduced-neutron width distribution for *p*-wave resonances in cesium up to 120 eV compared to the Porter-Thomas distribution.

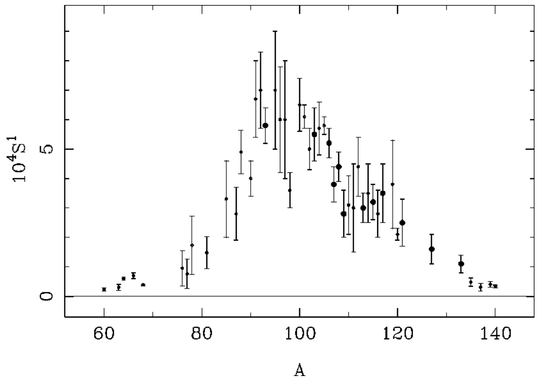

FIG. 7. The *p*-wave neutron strength function S_1 versus mass number A in the region of the $3p$ maximum. TRIPLE data are presented by solid circles.

the $j=1/2$ component is expected to be relatively stronger than the $j=3/2$ component on the higher-mass side of the $3p$ maximum near $A=100$ and weaker on the lower-mass side. Also we note that in this mass region local fluctuations of the S_0 neutron strength function were observed and attributed to nuclear shell structure effects [25] and to the influence of (two-particle–one-hole) doorway states [26,27]. All this physics can be apropos for the PV in compound nuclei, having in mind local fluctuations in the mass dependence of the weak spreading width.

IV. PNC DATA ANALYSIS AND RESULTS

A. PNC data

Longitudinal asymmetries were determined using the fitting code FITXS with fixed resonance parameters which were obtained first by fitting to the summed $(+)$ and $(-)$ helicity spectra. We introduced asymmetries p^+ and p^- for the separate $+$ and $-$ helicity spectra by the definition $\sigma_p^{\pm}=\sigma_p(1+p^{\pm})$, and determined p^+ and p^- from the fits. The resulting longitudinal asymmetries p were determined from $p=(p^+-p^-)/(2+p^++p^-)$. Details concerning the application of the FITXS code to PV data are given by Crawford *et al.* [5]. For each *p*-wave resonance studied the PV longitudinal asymmetries from separate runs were histogrammed for positive and negative proton polarization to obtain a mean value of the asymmetry p and its uncertainty. An ex-

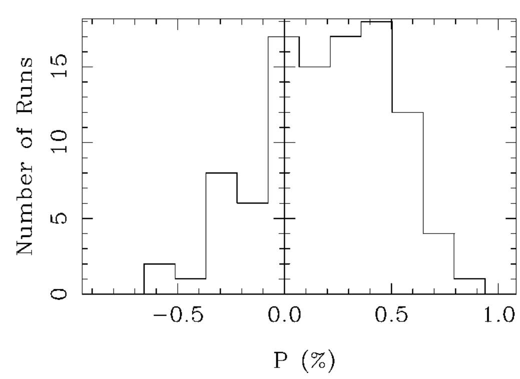

FIG. 8. Histogram of the longitudinal asymmetries for the 9.50-eV resonance obtained for each of 104 runs with positive proton polarization.

TABLE II. Longitudinal PNC asymmetries for neutron resonances in ^{133}Cs.

E_n (eV)	p (%)	$p/\delta p$
9.50	0.242 ± 0.023	10.4
16.77	-0.35 ± 0.47	-0.8
18.86	-0.28 ± 0.62	-0.5
19.98	-0.01 ± 0.14	-0.1
33.11	0.05 ± 0.30	0.1
42.75	-0.17 ± 0.18	-0.9
44.63	0.06 ± 0.15	0.4
58.09	1.20 ± 1.74	0.7
60.24	-0.08 ± 0.14	-0.5
78.52	-1.20 ± 1.35	-0.9
80.00	-0.17 ± 0.29	-0.6
88.96	-0.050 ± 0.03	-1.6
110.5	0.62 ± 0.44	1.4
115.2	0.02 ± 0.27	0.1
117.7	0.12 ± 0.23	0.5
119.9	0.05 ± 0.03	1.7
155.3	-0.070 ± 0.028	2.5
167.0	-0.08 ± 0.10	-0.8
267.5	-0.07 ± 0.08	-0.9
271.0	0.05 ± 0.20	0.2
273.6	-0.45 ± 0.50	-0.9
284.9	0.02 ± 0.06	0.3

ample of such a histogram is shown in Fig. 8 for the 9.50-eV resonance. The values of the longitudinal asymmetries determined for p-wave resonances in ^{133}Cs are listed in Table II.

B. PNC analysis and results

Finally, we constructed the Bayesian likelihood function L versus Γ_w using the asymmetries from Table II and Eq. (28) from the work of Bowman *et al.* [12]:

$$L(\Gamma_w)=\prod_i\left[\sum_{J=I\pm1/2}P^0(M_J)r(J)P^I(p_i|M_JA_i(J),a,\sigma_i)+\sum_{J=I\pm3/2}r(J)G(p_i,\sigma_i^2)\right],\qquad(6)$$

where M_J is expressed through Γ_w as $M_J=\sqrt{\Gamma_w D_J/2\pi}$. Here $P^0(M_J)$ is the *prior* probability density function for M_J, and the value $P^0(M_J)=1$ is assumed; $r(J)$ is the relative probability of spin J, $G(p_i,\sigma_i^2)$ is a Gaussian with experimental asymmetry p_i and corresponding uncertainty σ_i, the quantity a^2 is the ratio of the $p_{3/2}$ and $p_{1/2}$ neutron strength functions, and P^I is the appropriate probability density function discussed in detail in Ref. [12]. This expression holds for our particular case: s-wave spins known, most p-wave spins unknown, and the $j=1/2$ and $j=3/2$ projectile-spin amplitudes unknown. These uncertainties were accounted for in a statistical manner as described by Bowman *et al.* The value of the parameter a was taken to be 0.70 ± 0.10 [28]. The weak interaction mixes states of the opposite parity but with the same spin J. For a ^{133}Cs target (target spin $I=7/2$), p-wave neutrons excite compound states with spins $J=2$, 3, 4, or 5, while s-wave neutrons excite states with spins $J=3$ or 4. Resonances with $J=2$ and $J=5$ cannot mix with s-wave resonances. Therefore only the $J=3$ and $J=4$ states in the compound nucleus ^{134}Cs can exhibit PNC longitudinal asymmetries. Their contribution to $L(\Gamma_w)$ is accounted for by the first term in Eq. (6) while the second term corresponds to the $J=2$ and $J=5$ states. Since the spins of the p-wave resonances are not known, terms with all four possible J values occur in Eq. (6). The terms with $J=3$ and $J=4$ depend on M_J while terms with $J=2$ and $J=5$ do not. If a measured asymmetry is nonzero, then the terms with $J=2$ and $J=5$ play a small role. If a measured asymmetry is statistically consistent with zero, then all four terms are important. The nonzero asymmetry may be small because the matrix elements for the particular $J=3$ or $J=4$ states are small by chance. Application of Eq. (6) to the p-wave resonances with unknown spins requires knowledge of the spacings D_J. We used the values $D_{J=3}=47$ eV and $D_{J=4}=36$ eV which we obtained from $D_0=20.5$ eV by applying the $(2J+1)$ law for level densities.

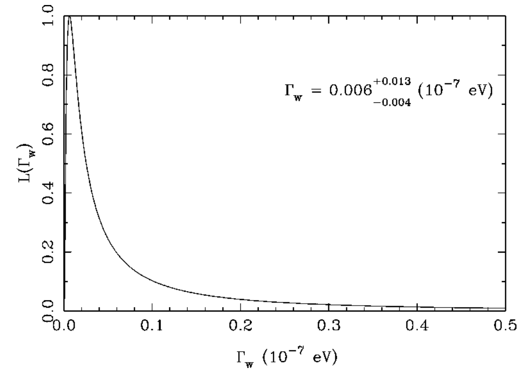

FIG. 9. Likelihood function L versus the weak spreading width Γ_w for p-wave resonances in ^{133}Cs. A spin $J=3$ is assumed for the 9.5-eV resonance. Indicated errors are from exp(-05) levels of likelihood.

The likelihood function with all p-wave resonance spins unknown is shown in Fig. 9. The maximum likelihood estimate and the 68% confidence interval obtained from this plot are

$$\Gamma_w=(0.006^{+0.154}_{-0.003})\times10^{-7}\ \text{eV}.\qquad(7)$$

The large value of the confidence interval in this result is due to only two statistically significant asymmetries and uncertainty in the A_i coefficients associated with unknown spins of resonances. The uncertainties in the A_j's associated with the uncertainties in other resonance parameters were not included because they were about 10% for each resonance and the likelihood analysis reduces their influence.

Neglecting any possible differences in M_J and D_J between states with $J=3$ and $J=4$, that is, using Eq. (3) with $D=2D_0=41$ eV, we obtain a value of the root-mean-square matrix element $M=(0.06^{+0.25}_{-0.02})$ meV. The likelihood function $L(\Gamma_w)$ has a relatively long tail. We could have chosen $z=\ln\Gamma_w$ as the independent variable in the likelihood analysis. The likelihood function for this choice is shown in Fig. 10. This likelihood function is more nearly symmetric than the likelihood function for Γ_w and to a good approximation

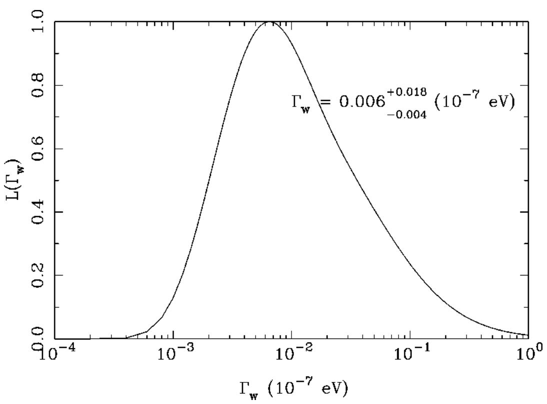

FIG. 10. Likelihood function L for the weak spreading width Γ_w for p-wave resonances in ^{133}Cs in the logarithmic representation. The spins of all p-wave resonances are unknown.

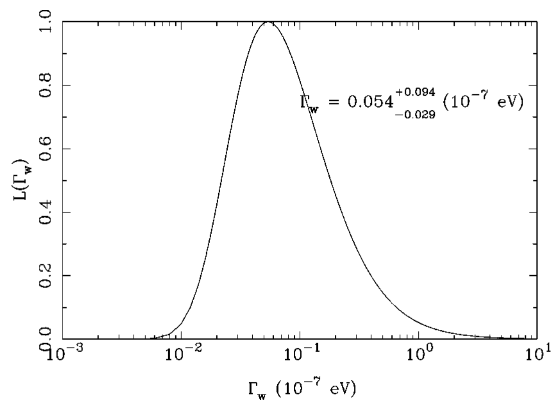

FIG. 11. Likelihood function L for the weak spreading width Γ_w for p-wave resonances in ^{133}Cs in the logarithmic representation. A spin $J=4$ is assumed for the 9.5-eV resonance.

the likelihood function $L(z)$ is Gaussian. Accepting the definition of standard error as for a Gaussian gives $z=\ln \Gamma_w=-5.12^{+1.39}_{-1.09}$ with Γ_w expressed in units of 10^{-7} eV. Spins $J=3$ and $J=4$ are both possible for the 9.5-eV resonance. For $J=3$, we obtain the same value as in Eq. (7) for the maximum likelihood estimate of Γ_w, although the function $L(\Gamma_w)$ is narrower than in Fig. 9. For $J=4$, we obtain the likelihood function shown in Fig. 11. The larger value of the maximum likelihood estimate in this case is due to the smaller $A_{J=4}$ value (see Table I) as compared to the $J=3$ case. The maximum is inside the 68% confidence interval for the value of Eq. (7). However, a spin assignment for the 9.5-eV p-wave resonance would be useful.

V. SUMMARY

With the polarized pulsed neutron beam at LANSCE, we have measured transmission through a thick cesium sample and observed for the first time many p-wave resonances in the neutron energy range of 5–400 eV. We measured the neutron widths and determined the p-wave strength function $S_1=(1.1\pm 0.3)\times 10^{-4}$, which is the smallest value of S_1 measured by the TRIPLE Collaboration. The PNC longitudinal asymmetries were obtained for 22 p-wave resonances in the energy range up to 285 eV. Parity violation is observed at the 9.50-eV resonance with 10σ statistical significance and at the 155-eV resonance with 2.5σ statistical significance. The other p-wave resonances that did not show any PNC effect are also important in establishing the weak matrix element because PNC amplification parameters are large for many of them. The values of the root-mean-square PNC element $M=(0.06^{+0.25}_{-0.02})$ meV and the weak spreading width $\Gamma_w=(0.008^{+0.154}_{-0.003})\times 10^{-7}$ eV in ^{133}Cs are the smallest of all the targets studied by the TRIPLE Collaboration. These results together with similar conclusions from PNC results for niobium [9] provide additional evidence that there exist local fluctuations in the mass dependence of the weak interaction in compound nuclei. More detailed study including spins and $S_{1/2}, S_{3/2}$ strength function measurements for p-wave resonances is needed to understand this behavior.

ACKNOWLEDGMENTS

This work was supported in part by the U.S. Department of Energy, Office of High Energy and Nuclear Physics, under Grants No. DE-FG02-97-ER41042 and DE-FG02-97-ER41033. The work was performed at the Los Alamos Neutron Science Center at the Los Alamos National Laboratory. This facility is funded by the U.S. Department of Energy, Office of Energy Research, under Contract W-7405-ENG-36.

[1] G. E. Mitchell, J. D. Bowman, and H. A. Weidenmüller, Rev. Mod. Phys. (to be published).

[2] V. P. Alfimenkov, S. B. Borzakov, Vo Van Thuan, Yu. D. Mareev, L. B. Pikelner, A. S. Khrykin, and E. I. Sharapov, Nucl. Phys. **A398**, 93 (1983).

[3] J. D. Bowman, G. T. Garvey, Mikkel B. Johnson, and G. E. Mitchell, Annu. Rev. Nucl. Part. Sci. **43**, 829 (1993).

[4] C. M. Frankle, S. J. Seestrom, Yu. P. Popov, E. I. Sharapov, and N. R. Roberson, Fiz. Elem. Chastits At. Yadra **24**, 939 (1993) [Phys. Part. Nuclei **24**, 401 (1993)].

[5] B. E. Crawford *et al.*, Phys. Rev. C **58**, 1236 (1998).

[6] S. L. Stephenson *et al.*, Phys. Rev. C **58**, 1225 (1998).

[7] S. J. Seestrom *et al.*, Phys. Rev. C **58**, 2977 (1998).

[8] L. Y. Lowie *et al.*, Phys. Rev. C **59**, 1119 (1999).

[9] E. I. Sharapov *et al.*, Phys. Rev. C **59**, 1131 (1999).

[10] J. D. Bowman *et al.*, Phys. Rev. Lett. **65**, 1192 (1990).

[11] H. A. Weidenmüller, *Fundamental Symmetries in Nuclei and Particles*, edited by H. Henriksen and P. Vogel (World Scientific, Singapore, 1990), p. 30.

[12] J. D. Bowman, L. Y. Lowie, G. E. Mitchell, E. I. Sharapov, and Yi-Fen Yen, Phys. Rev. C **53**, 285 (1996).

[13] A. Bohr and B. R. Mottelson, *Nuclear Structure I* (W. A. Benjamin, New York, 1969).

[14] H. L. Harney, A. Richter, and H. A. Weidenmüller, Rev. Mod. Phys. **58**, 607 (1986).

[15] S. F. Mughabghab, M. Divadeenam, and N. E. Holden, *Neutron Cross Sections* (Academic Press, New York, 1981).

[16] V. A. Anufriev, T. S. Belanova, C. I. Babich, Yu. S. Zamyat-

nin, A. G. Kolesov, E. I. Shkokov, S. M. Kalebin, V. S. Artamonov, and P. N. Ivanov, At. Energ. **43**, 201 (1977) [Sov. At. Energy **43**, 828 (1977)].
[17] P. W. Lisowski, C. D. Bowman, G. J. Russell, and S. A. Wender, Nucl. Sci. Eng. **106**, 208 (1990).
[18] V. W. Yuan *et al.*, Phys. Rev. C **44**, 2187 (1991).
[19] J. D. Bowmam, Y. Matsuda, Y.-F. Yen, and B. E. Crawford, computer code FITXS for analysis of neutron time-of-flight spectra, 1997 (unpublished).
[20] Y. Matsuda, Ph.D. thesis, Kyoto University, Report No. KUNS-1492, 1998.
[21] B. E. Crawford *et al.*, Phys. Rev. C **58**, 729 (1998).
[22] C. W. Reich and M. S. Moore, Phys. Rev. **111**, 929 (1958).
[23] L. M. Bollinger and G. E. Thomas, Phys. Rev. **171**, 1293 (1968).
[24] H. S. Camarda, Phys. Rev. C **9**, 28 (1974).
[25] A. M. Lane, J. E. Lynn, E. Melkonian, and E. R. Rae, Phys. Rev. Lett. **2**, 424 (1959).
[26] C. Shakin, Ann. Phys. (N.Y.) **22**, 373 (1963).
[27] H. Feshbach, A. K. Kerman, and R. H. Lemmer, Ann. Phys. (N.Y.) **41**, 230 (1967).
[28] L. V. Mitsyna, A. B. Popov, and G. S. Samosvat, in *Nuclear Data for Science and Technology*, edited by S. Igarasi (Saikon, Tokyo, 1988), p. 111.